ISSN 0036-0244, Russian Journal of Physical Chemistry A, 2014, Vol. 88, No. 3, pp. 494–502. © Pleiades Publishing, Ltd., 2014.
Original Russian Text © I.K. Razumov, 2014, published in Zhurnal Fizicheskoi Khimii, 2014, Vol. 88, No. 3, pp. 458–494.

PHYSICAL CHEMISTRY
OF NANOCLUSTERS AND NANOMATERIALS

Grain Boundary Segregations in Nanocrystalline Alloys

I. K. Razumov
Institute of Metal Physics, Ural Branch, Russian Academy of Sciences, Yekaterinburg, Russia
e-mail: rik@imp.uran.ru

Received June 1, 2013

Abstract—The dependence of grain boundary segregations and alloy composition in the bulk of the grain on the grain size was considered. At moderate temperatures, there is a critical grain size for which the integrated degree of alloy decomposition reaches its maximum; this size increases as the average (over the sample) impurity concentration decreases. In complex alloys, the type of the component that segregates on the boundaries depends on the grain size. For segregation kinetics, an approximate analytical solution was obtained based on the assumption that the grain boundary is an ideal drain for the impurity. The equilibrium grain size exists below the critical temperature and its temperature dependence is nonmonotonic in the general case. A segregation mechanism of stabilization of nonequilibrium grain boundaries in nanocrystalline alloys obtained by severe plastic deformation was suggested.

Keywords: nanocrystalline alloys, segregation, critical grain size, kinetics, critical temperature.

DOI: 10.1134/S0036024414030212

INTRODUCTION

Grain boundary segregations (GBSs) determine many performance characteristics of materials, primarily, their strength, plasticity, and creep [1, 2] and electric properties [3, 4]. They also affect the reliability and service time of equipment [5, 6] and the grain size achieved after severe plastic deformation (SPD) [7–9]. They also facilitate the development of phase instability [10]. In ultradisperse systems in which the fraction of near-boundary atoms is comparable to that of atoms in the bulk, GBSs considerably change the thermodynamics of alloys; as a result, the traditional phase diagrams of alloys are suitable only in a local sense [11–13].

According to the mechanism of their formation and characteristic properties, segregations are divided into equilibrium and nonequilibrium ones [14]. Equilibrium segregations result from a change in the chemical potential of atoms on the free surface [15] or boundaries of grains [16]. In the latter case, they are stable to the same extent as the grain structure. The steady state of these segregations is described by Langmuir–McLean [17] and Fowler [18] isotherms. The formation kinetics is described by the McLean [17] and Slezov [19] equations. In contrast, nonequilibrium segregations appear only at the intermediate stages of kinetics generally as a result of the treatment of the substance and disappear after prolonged annealing. Nonequilibrium segregations appear during irradiation [20] and probably during SPD as a result of the action of vacancy [21] or dislocation flows [22, 23].

Nanocrystalline alloys obtained by SPD have long ago attracted the attention of researchers in view of prospects for technological application [24–26], but the nature of phase transformations in them [27–34] remains debatable. On the one hand, a strong mechanical action is believed to cause "frozen" nonequilibrium phase states [35–37], including nonequilibrium GBSs. On the other hand, it gives rise to so-called nonequilibrium grain boundaries with excess dislocations [24] and a small grain size is achieved at which the proportion of near-boundary atoms is comparable to the bulk proportion. If the grain boundary (GB) is assumed to be 1 nm, there are is 25% near-boundary atoms for 10 nm grains and 50% for 5 nm grains [38]. The latter suggests that equilibrium GBSs make a considerable contribution to the picture of phase transformations during SPD [11–13]. To understand the general picture, it is necessary to study the possible results of the action of various mechanisms.

Though the subject seems very simple, the equilibrium GBSs in grains with finite dimensions were studied insufficiently and the most important studies (e.g., [19, 39]) are not well-known. A theoretical rationale for the similarity of kinetics and degree of segregation on a free surface and intergrain boundaries was given in [40] and experimental support for this was published in [41, 42]; it was concluded that these quantities can be described in terms of the same theory. The results of the experiments of [43, 44] were important, from which it followed that GBSs can cover several atomic layers. An approximate equation for the segregation kinetics was derived in [19] for alloys with unlimited solubility and studied further in an assumption that the impurity concentration in the bulk of the grain remains small, but increases considerably at the grain boundary [45]. It follows from this solution that the concentration of the segregating component on the GBs decreases with the grain size and the segregation kinetics can be nonmonotonous due to the difference between the diffusion coefficients and segregation energies of impurity atoms. It was shown [39] that for binary alloys at critical temperatures, there is a critical grain size starting from which the whole impurity segregates at the GBs and is completely removed from the bulk of the grain. It was also shown that the dependence of the impurity concentration on the GB on the grain size in ternary systems can be nonmonotonous. Studies of the effect of the grain size on the development of a GB phase transition, which is possible on condition of interaction between the atoms of the segregated component, were reported in [46]. It was shown that as the grain size decreases, the GB phase transition shifts toward lower temperatures. This effect is a simple consequence of the decrease in the concentration of the segregated component on the GB when the grain size decreases. A numerical simulation of the joint kinetics of segregations and decomposition in finite-size grains was performed [11–13] using a regular solid solution model [47]. It was shown that the degree of stability of an alloy in the bulk of grains changes in view of redistribution of atoms between the GB and the volume. It was predicted [48] that the grain structure can be stabilized due to a decrease in the energy of intergrain boundaries during the impurity segregation. For Ni–P and Ni–W systems, this effect was well supported experimentally [8].

Here, we reviewed possible effects in the development of GB segregations depending on the grain size and predicted new qualitative features of transformations in nanocrystalline materials to elaborate the above concepts. Thus the integrated degree of decomposition is an important characteristic of an alloy, which shows the degree of nonhomogeneity of the alloy in composition and affects its electric and magnetic properties. It follows from a combined analysis of the conditions of the Gibbs equilibrium and the law of conservation of matter that the dependence of this characteristic on the grain size is a nonmonotonous function so that there is a critical grain size at which the degree of decomposition is maximum.

Another important characteristic is the impurity concentration on the grain boundary, which largely determines the mechanical properties of the material. As shown in [39], the behavior of this characteristic qualitatively changes when a certain critical size is reached. It seems useful to compare these two definitions of the critical size and consider their temperature dependence. For early stages of the segregation kinetics, a simple approximate solution was proposed, which seems especially useful for multicomponent systems; this solution was compared with Slezov kinetics. Finally, it was shown that with GB segregations, the equilibrium grain size exists only below the critical temperature and that the temperature dependence of this size is generally nonmonotonous and qualitatively different for dilute and saturated solid solutions. It was hypothesized that for nanocrystalline alloys obtained by SPD the appearance of nonequilibrium GBs hinders further size reduction of grains because the equilibrium grain size increases due to the larger segregation capacity of these boundaries. The stated peculiarities of the thermodynamics of nanocrystalline alloys should be taken into account in the design of new promising materials.

Critical Grain Size in Binary Alloys

Let us consider a grain shaped as a sphere of a radius L with a boundary layer with a width d. Suppose the grain has an equilibrium distribution of concentrations so that the impurity concentration on the grain boundary is c_{GB} and the impurity concentration in the bulk is c_b. Then the law of conservation of matter has the form

$$c_b\left(L-d\right)^3+c_{GB}\left(L^3-\left(L-d\right)^3\right)=c_0L^3, \tag{1}$$

where c_0 is the average impurity concentration over the grain.

For the regular solid solution model [47], the concentrations c_{GB} and c_b are related by the Fowler equation [18]

$$\frac{c_{\mathrm{GB}}}{(1-c_{\mathrm{GB}})}=\frac{c_b}{(1-c_b)}\exp\left[\frac{\delta\varepsilon-\delta\nu/2+\nu_bc_b-\nu_{\mathrm{GB}}c_{\mathrm{GB}}}{kT}\right], \tag{2}$$

where $\delta\varepsilon=\varepsilon_b-\varepsilon_{\mathrm{GB}}$, $\delta\nu=\nu_b-\nu_{\mathrm{GB}}$ are the changes in the dissolution and mixing energies of the impurity on the GB relative to the corresponding energies in the bulk; ε_b, $\varepsilon_{\mathrm{GB}}$ are the dissolution energies; ν_b, ν_{GB} are the mixing energies in the bulk and on GB; and $-\delta\varepsilon$ is the segregation energy. The Fowler equation appears from the condition of equality between the chemical potentials at equilibrium, $\mu_{\mathrm{GB}}=\mu_b$, where $\mu=\delta f/\delta c$, and the free energy density of the alloys is

$$f(c)=f_0+\varepsilon c-\frac{\nu}{2}c(1-c)+kT\left[c\ln c+\left(1-c\right)\ln(1-c)\right].$$

If the composition of alloy c_0 and the energy parameters in the bulk and on the GB are known, (1) and (2) form a system for the concentrations c_{GB} and c_b. The system has a physically adequate solution at temperatures above the decomposition line recorded as

$$kT/\nu=(1-2c)\left[\ln\left(c/(1-c)\right)\right]^{-1}.$$

For the ideal solution ($\nu_{\mathrm{GB}}=\nu_b=0$), Eq. (2) is called the Langmuir–McLean isotherm [17]. The solution of system (1), (2) for this case is of the form

$$c_{\mathrm{GB}}(L)=\frac{2c_0\left(\tilde{\varepsilon}+1\right)}{1+q+\tilde{\varepsilon}\left(p+c_0\right)},$$

$$c_b(L)=-\frac{1-q+\left(p-c_0\right)\tilde{\varepsilon}}{2\tilde{\varepsilon}\left(1-\tilde{d}\right)^3}, \tag{3}$$

$$q=(4c_0(1-\tilde{d})^3\tilde{\varepsilon}+[c_0+(1-\tilde{d})^3+(p-c_0)(1+\tilde{\varepsilon})]^2)^{1/2},$$

where $\tilde{d} = d/L$, $\tilde{\varepsilon} = \exp[\delta\varepsilon/kT] - 1$, and $p = 3\tilde{d} - 3\tilde{d}^2 + \tilde{d}^3$. This solution has never been recorded in analytical form because the formulas are cumbersome. However, the analytical form of the solution is useful in several problems, for example, when seeking an equilibrium grain size.

The integrated degree of decomposition is recorded as

$$S_d = \frac{1}{2c_0(1-c_0)V}\int |c(\mathbf{r}) - c_0|\, d\mathbf{r}, \qquad (4)$$

where V is the volume of the sample. S_d can take values from 0 to 1. It characterizes the macroscopic properties of the material and is useful for interpreting the experiments in which the decomposition is recorded on the basis of indirect signs (magnetic susceptibility of the sample, magnetization, change in the mean lattice parameter, etc.). For a grain shaped as a sphere with a radius L with a near-boundary layer with a width d, we have

$$S_d = \frac{(1 - d/L)^3 (c_0 - c_b)}{c_0(1 - c_0)}. \qquad (5)$$

Figures 1 and 2 show the dependences of the concentrations c_b and $c_{\rm GB}$ on the grain size at a fixed GB (in the adopted notation, L is half of the grain size and d is the half-width of the GB). The alloy considered ideal; the only energy parameter $\delta\varepsilon/kT$ at fixed $\delta\varepsilon$ determines the temperature. We can see that in the limit of low temperatures (i.e., $\delta\varepsilon/kT \gg 1$; curves *1* and *2*, Fig. 1), the decrease in the grain size is accompanied by a monotonic decrease in c_b to a certain critical size at which the grain is ideally purified from the impurity ($c_b = 0$). The impurity concentration on the boundary $c_{\rm GB}$ at $L > L_{\rm cr}$ is nearly constant (curves *1* and *2*, Fig. 2) at $L > L_{\rm cr}$ and decreases monotonically with the grain size at $L < L_{\rm cr}$. This decrease is caused by the exhaustion of the impurity in the bulk and its uniform distribution over the whole area of boundaries according to model assumptions. An increase in T leads to a smoothing of the curves, which remains insignificant within a reasonable range of parameters (curves *1*' and *2*'). For random temperatures, it is reasonable to determine the critical size $L_{\rm cr}^{(1)}$ from the inflection point on the $c_b(L)$ curve. For $L < L_{\rm cr}^{(1)}$, the limiting grain boundary impurity concentrations $c_{\rm GB}$ no longer depend on the sort of the impurity or temperature and depend only on the grain size (in Fig. 2, curves *1* and *1*', *2* and *2*' come closer to each other at $L/d \to 1$). The effect of decreasing $c_{\rm GB}$ at smaller grain sizes is well known [19, 14] and was supported experimentally [49]. The existence of a clear-cut critical size $L_{\rm cr}^{(1)}$ was discussed in [39], but the dependence of $L_{\rm cr}^{(1)}$ on the parameters (e.g., temperature) of the problem was not considered.

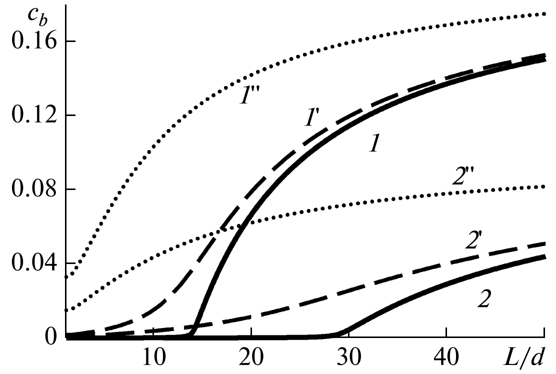

Fig. 1. Dependences of the equilibrium impurity concentration in the bulk of grain on the grain size at $c_0 = 0.20$ (*1*, *1*', *1*''), 0.10 (*2*, *2*', *2*'') and different perturbations on the boundary: $\delta\varepsilon/kT = 10$ (*1*, *2*), 5 (*1*', *2*'), and 2 (*1*'', *2*'').

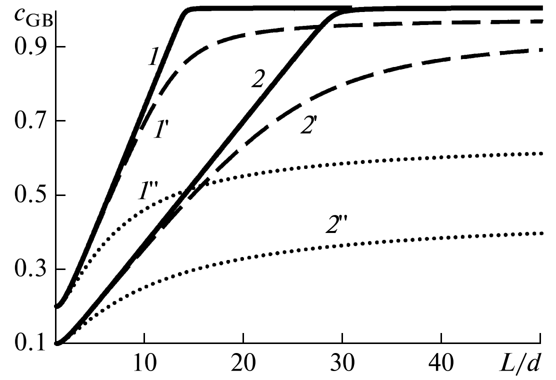

Fig. 2. Dependences of the equilibrium GB impurity concentration on the grain size. For notation, see Fig. 1.

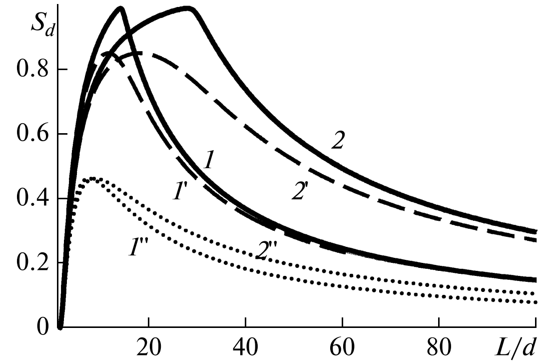

Fig. 3. Dependences of the integrated degree of decomposition on the grain size. For notation, see Fig. 1.

Figure 3 presents the plots of the integrated degree of decomposition $S_d(L)$ on the grain size at the same parameters. It can be seen that the $S_d(L)$ curve has a maximum whose position can be correlated with another critical size, $L_{\rm cr}^{(2)}$. The critical sizes $L_{\rm cr}^{(1)}$ and $L_{\rm cr}^{(2)}$

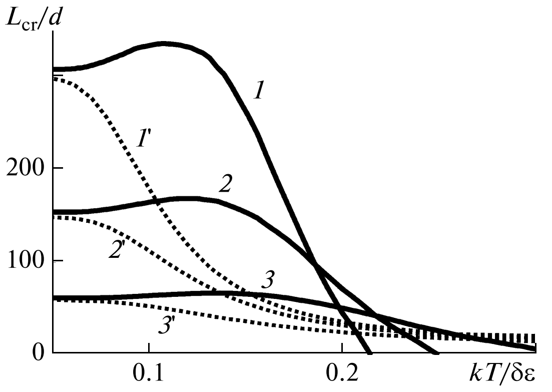

Fig. 4. Temperature dependences of the critical sizes $L_{cr}^{(1)}$ (*1–3*) and $L_{cr}^{(2)}$ (*1'–2'*) at $c_0 = 0.01$ (*1*, *1'*), 0.02 (*2*, *2'*), and 0.05 (*3*, *3'*).

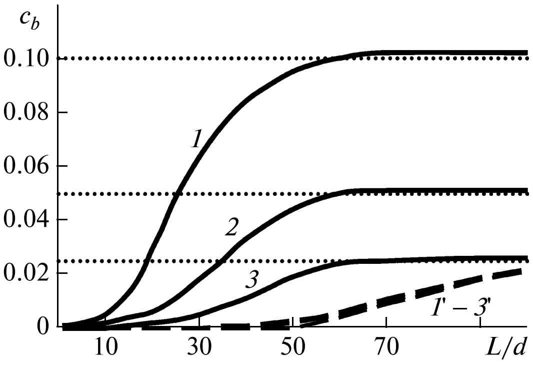

Fig. 5. Dependences of the equilibrium impurity concentrations in the bulk of grain $c_b^{(1)}$ (*1–3*) and $c_b^{(2)}$ (*1'–3'*) on the grain size in a ternary alloy at $\delta\varepsilon^{(1)}/kT = 5$, $\delta\varepsilon^{(2)}/kT = 10$, $c_0^{(2)} = 0.05$; $c_0^{(1)} = 0.10$ (*1*), 0.05 (*2*), and 0.025 (*3*). The dotted lines denote the levels of the uniform distribution, $c_0^{(1)}$.

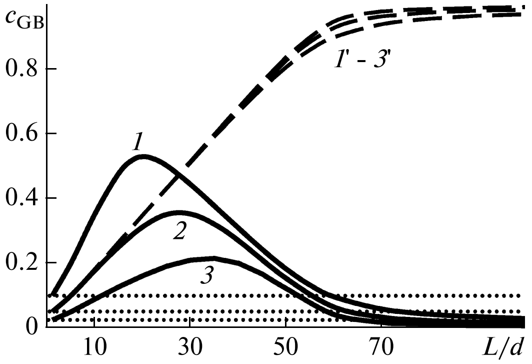

Fig. 6. Dependences of the equilibrium grain boundary impurity concentrations $c_{GB}^{(1)}$ (*1–3*) and $c_{GB}^{(2)}$ (*1'–3'*) on the grain size in a ternary alloy. For notation, see Fig. 5.

do not coincide at a random temperature, but approach each other in the limit of low temperatures. The plots of the temperature dependences $L_{cr}^{(1)}(T)$ and $L_{cr}^{(2)}(T)$ at different impurity concentrations c_0 are shown in Fig. 4. It can be seen that the critical size $L_{cr}^{(1)}$ exists only below a certain threshold temperature, which decreases with c_0, while $L_{cr}^{(2)}$ exists at any arbitrarily high temperature. Both critical sizes quickly increase as c_0 decreases, reaching hundreds of nanometers already at $c_0 = 0.01$.

For spherical grains, the properties of GBs are the same over the whole grain surface. The real grain structure, however, contains boundaries of different (small- and large-angle) types, and the flat regions of GBs alternate with regions of ternary joints of grains, where the perturbations $\delta\varepsilon$, $\delta\nu$ are more pronounced. This suggests a hierarchy of critical sizes at which the properties of materials change significantly. For example, the volume fraction of atoms lying at ternary joints naturally increases as L decreases. This suggests the existence of a critical size $L_{cr}^{(3)}$ for highly dilute solid solutions, at which both the volume and the GB are ideally purified from the impurity so that all impurity atoms assemble at ternary joints.

Grain Boundary Segregations in Ternary Systems

In an approximation of the ideal solid solution, the free energy density of a multicomponent alloy is

$$f(\{c^{(i)}\}) = \sum_{i=1}^{N}(\varepsilon^{(i)}c^{(i)} + kTc^{(i)}\ln c^{(i)}) + kT\left[\left(1-\sum_{i=1}^{N}c^{(i)}\right)\ln\left(1-\sum_{i=1}^{N}c^{(i)}\right)\right], \quad (6)$$

where N is the number of impurity sorts; $\varepsilon^{(i)}$ and $c^{(i)}$ are the energy of dissolution and the concentration of the ith impurity. Then, by analogy with (1) and (2), the system

$$c_b^{(i)}(1-d/L)^3 + c_{GB}^{(i)}\left(1-(1-d/L)^3\right) = c_0^{(i)}, \quad (7)$$

$$c_{GB}^{(i)}\left(1-\sum_{i=1}^{N}c_b^{(i)}\right) = c_b^{(i)}\left(1-\sum_{i=1}^{N}c_{GB}^{(i)}\right)\exp\left[\frac{\delta\varepsilon^{(i)}}{kT}\right] \quad (8)$$

is valid.

Figures 5 and 6 present a typical solution of this system for a ternary alloy for different grain sizes. In large grains on the GB, the component with large $\delta\varepsilon$ segregates irrespective of the average concentration of another impurity (curves *1'–3'*, Fig. 6), which can decrease on the GB (*1–3*, Fig. 6), but remains almost constant in the bulk of the grain (*1–3*, Fig. 5). Thus the component with smaller $\delta\varepsilon$ is blocked in the bulk of large grains under the thermodynamic equilibrium conditions.

When the grain size decreases to the critical value $L_{\mathrm{cr}}^{(1)}$, the component with large $\delta\varepsilon$ in the bulk is exhausted due to segregation on the GB (*1'–3'*, Fig. 5); therefore, the concentration of this component on the GB decreases as the grain size decreases further (*1'–3'*, Fig. 6). As a result, the component with smaller $\delta\varepsilon$ can segregate on the GB. Therefore, for the component with a smaller $\delta\varepsilon$ value, the $c_{\mathrm{GB}}(L)$ dependence is nonmonotonic (*1–3*, Fig. 6), while $c_b(L)$ is a threshold dependence (*1–3*, Fig. 5). The calculations show that these qualitative features of segregations, including the nonmonotonic character of the $c_{\mathrm{GB}}(L)$ dependence for the component with a smaller $\delta\varepsilon$ value, persist at lower concentrations $c_0^{(i)}$ when the maximum grain boundary concentrations $c_{\mathrm{GB}}^{(i)}$ are no longer close to 1. This effect was mentioned in [39] and is given here mainly for the sake of a comprehensive review.

Kinetics of Grain Boundary Segregations

A system of algebraic equations for GBS kinetics was suggested by Slezov et al. [19, 45]. This system is based on a reasonable assumption that the grain boundary is rather narrow and the diffusion coefficient on it is large compared with that in the bulk. Therefore, the local thermodynamic equilibrium sets in on the GB within the times that are much smaller than the characteristic segregation kinetics times determined by the impurity diffusion from the bulk. This allows us to use the Fowler equation (2) or the Langmuir–McLean isotherm at an arbitrary stage of kinetics for correlating the impurity concentrations on the grain boundary $c_{\mathrm{GB}}(t)$ and in the neighboring layer $\lambda(t)$. In the ideal solid solution approximation for the spherical grain, the system has the form

$$c_{\mathrm{GB}}^{(i)}(t) = c_0^{(i)} + \frac{2}{\pi^2}\left(\frac{L}{d}-1\right)\left(c_0^{(i)} - \lambda^{(i)}(t)\right)S(t),$$
$$S(t) = \sum_{n=1}^{\infty}\frac{1}{n^2}\left[1-\exp\left(-\frac{D^{(i)}\pi^2n^2}{(L-d)^2}t\right)\right], \tag{9}$$

$$c_{\mathrm{GB}}^{(i)}(t)\left(1-\sum_{i=1}^{N-1}\lambda^{(i)}(t)\right) = \lambda^{(i)}(t)\left(1-\sum_{i=1}^{N-1}c_{\mathrm{GB}}^{(i)}(t)\right)\exp\left(\frac{\delta\varepsilon^{(i)}}{kT}\right). \tag{10}$$

The solution of this system for the binary alloy is as follows (it was not given in [19, 45] probably because of the cumbersome form of the formulas):

$$c_{\mathrm{GB}}(t) = -\frac{p+q}{2\tilde{\varepsilon}},$$
$$p = c_0 + \left(\tilde{S}(t)-1\right)(c_0-1) - (\tilde{\varepsilon}+1)\left(1+c_0+c_0\left(\tilde{S}(t)-1\right)\right),$$
$$q = [-4c_0\tilde{\varepsilon}(\tilde{\varepsilon}+1)\tilde{S}(t) + (\tilde{\varepsilon}+\tilde{S}(t)+c_0\tilde{\varepsilon}\tilde{S}(t))^2]^{1/2}, \tag{11}$$
$$\tilde{\varepsilon} = \exp[\delta\varepsilon/kT]-1,$$
$$\tilde{S}(t) = 1 + S(t)\left(L/d-1\right).$$

It is difficult to find an analytical solution of system (9), (10) for a multicomponent alloy. Therefore, we should seek approximate solutions.

Note that the impurity segregation energies are generally large compared with the thermal energy, $\delta\varepsilon^{(i)}/kT \gg 1$. For example, the Ag segregation energy on the grain boundaries in the γFe–40 wt % Ni was evaluated at –47 kJ/mol [50], which is approximately five times higher than the thermal energy at T = 1000 K. The experimental data and numerous theoretical predictions, which showed that the segregation energy of B, P, S, Sb, and Sb in α-Fe is approximately the same, were summarized in [14]. Hence it follows that at the initial stages of kinetics, the grain boundary acts as an ideal drain for impurities; i.e., $\lambda^{(i)}(t) \approx 0$. Due to this, at $\lambda^{(i)}(t) = 0$, (9) is considered the final solution independent of (10).

An equation that is close to (9) in form for $\lambda^{(i)}(t) = 0$ can be derived in a simple alternative way. Indeed, it follows from the law of conservation of matter that

$$\frac{4}{3}\pi[L^3-(L-d)^3](c_{\mathrm{GB}}^{(i)}(t)-c_0^{(i)}) = \int(c_0^{(i)}-c^{(i)}(r,t))d\nu. \tag{12}$$

Integration is performed here over the volume of a sphere with a radius $R = L - d$; $c^{(i)}(r,t)$ is a reference solution for the inner region of the sphere with a boundary condition $c^{(i)}(R,t) = \lambda^{(i)}(t) = 0$ [51]:

$$c^{(i)}(r,t) = c_0^{(i)}\frac{2R}{\pi r}\sum_{n=1}^{\infty}\frac{(-1)^{n+1}}{n}\sin\left(\frac{\pi n r}{R}\right) \times\exp\left(-\frac{D^{(i)}\pi^2n^2t}{R^2}\right). \tag{13}$$

Calculating the integral in (12), taking into account (13), we obtain

$$c_{\mathrm{GB}}^{(i)}(t) = \frac{c_0^{(i)}}{1-(1-d/L)^3} \times\left[1-\frac{6(1-d/L)^3}{\pi^2}\sum_{n=1}^{\infty}\frac{1}{n^2}\exp\left(-\frac{D^{(i)}\pi^2n^2t}{L^2(1-d/L)^2}\right)\right]. \tag{14}$$

Taking into account that $\sum_{n=1}^{\infty}1/n^2 = \pi^2/6$, we can easily verify that (14) coincides with (9) at $\lambda^{(i)}(t) = 0$ in the first term of the expansion in terms of the small parameter d/L.

In this sense, in the limit of $\delta\varepsilon^{(i)}/kT \gg 1$, $t \to 0$, Eq. (14) is more precise than (9) for calculating the dependence of the segregation kinetics on the grain size.

When the GB is saturated with the impurity, it ceases to be an ideal drain and the condition $\lambda^{(i)}(t) = 0$ is violated. Consequently, the accuracy of the rough

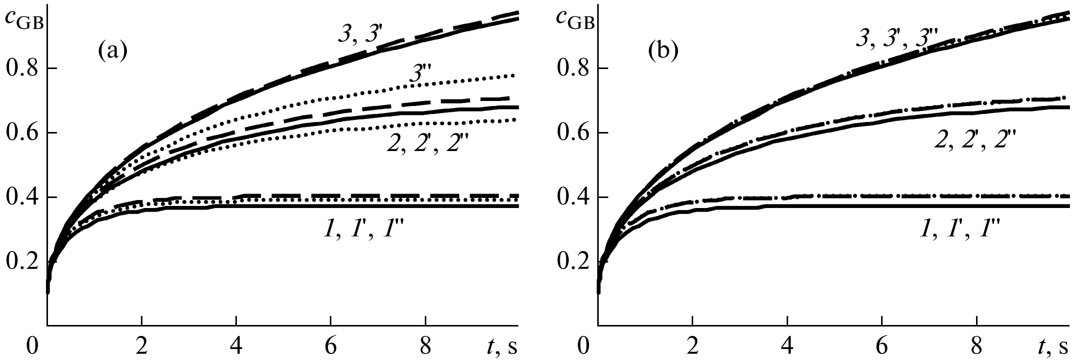

Fig. 7. Kinetics of GBSs in a binary alloy at $c_0 = 0.1$, $D = 10^{-17}$ m^2/s, $d = 1$ nm, $L/d = 10$ (*1*, *1'*, *1''*), 20 (*2*, *2'*, *2''*), and 40 (*3*, *3'*, *3''*); $\delta\varepsilon/kT = 5$ (Fig. 7a) and $\delta\varepsilon/kT = 10$ (Fig. 7b). The solutions were obtained by Eqs. (14) (solid lines), (9) at $\lambda = 0$ (dashed line), and (11) (dotted lines).

solution (14) decreases near the equilibrium concentrations, which can be found by Eq. (3) for a binary alloy or by solving system (7), (8) for a multicomponent alloy. A more adequate approximate solution can be obtained by sewing together the solution of (14) at small times with the indicated equilibrium concentrations in the limit of large times. For the binary alloy, it is reasonable to perform the sewing by choosing the smaller of the two solutions.

The situation for the multicomponent alloy is less trivial; in view of the difference between the diffusion coefficients of impurities, the concentration of a certain impurity on the GB can at first increase to high values and then decrease because of its withdrawal by another impurity as the latter comes to the GB [45]. The competition between impurities on the GB leads to additional limitation of the applicability of (14): the sum of impurity concentrations on the GB should not exceed 1. Therefore, it is reasonable to note that this condition is necessarily satisfied starting from a certain size $L < L_{cr}^{(1)}$ because of the decrease in the equilibrium $c_{GB}^{(i)}(L)$ at smaller grain sizes (Fig. 2); i.e., Eq. (14) is adequate for multicomponent nanocrystalline alloys.

Figure 7 presents for comparison the plots of segregation evolution calculated by Eqs. (9) for $\lambda(t) = 0$, (11), and (14) for grains with different sizes in a binary alloy. We can conclude that in nanocrystalline alloys (or, more precisely, when $L < L_{cr}^{(1)}$), Eq. (14) remains adequate even in the saturation mode (curves *1* and *2*, Fig. 7a). This is caused by the fact that at $L < L_{cr}^{(1)}$, the grain boundary continues to act as an ideal drain of an impurity until the impurity is exhausted in the bulk of the grain. Indeed, according to Figs. 1 and 2, after the equilibrium set in at $L < L_{cr}^{(1)}$, the impurity concentration in the bulk is close to zero (in particular, the condition $\lambda^{(i)}(t) = 0$ is satisfied), while the impurity concentration on the GB is far from unity. Consequently, if both conditions $L < L_{cr}^{(1)}$ and $\delta\varepsilon/kT \gg 1$ are satisfied in a binary alloy, there are no limitations on the applicability of (14) even at late stages of the kinetics. This actually means that the grain boundary impurity concentrations $c_{GB}(t)$ depend on the sort of the substance and the temperature only at the initial stages of the kinetics via the diffusion coefficient and mainly on the grain size at the last stages.

A comparison of Figs. 7a and 7b shows that the accuracy of solution increases with $\delta\varepsilon/kT$ so that at $\delta\varepsilon/kT \approx 10$, the solution is considered valid up to $c_{GB} = 1$ irrespective of the grain size. On the other hand, the minor difference between the solution of (14) from that of (11) at a small grain size is due to the above-mentioned larger nonlinearity of (14) according to the d/L parameter. This follows from the fact that in the limit of large $\delta\varepsilon/kT$, the solutions of (14) and (11) coincide for large grains but still differ for small ones (Fig. 7b).

Grain Boundary Phase Transition

For a regular solid solution, the possibility of a GB phase transition follows from the fact that when a spinodal is reached at a local level due to the condition $1 - 2\nu c(1 - c) = 0$, anomalous (ascending) diffusion takes place in the system [52]; i.e., the diffusion coefficient of impurities becomes negative. The Fowler isotherm (2) takes the characteristic form, becoming *S*-like, so that one temperature corresponds to different c_{GB} values [14]; that is, the solution is disrupted. An analysis of grain size effects using the Fowler isotherm was reported in [46]. It was shown that the GB phase transition is shifted toward lower temperatures at smaller grain sizes and the achieved GB concentration decreases because the impurity is distributed over the whole boundary.

The latter conclusion is wrong because when a small grain size is achieved, the Fowler equation is inapplicable to a description of the GB transition. Indeed, the GB phase transition starts according to

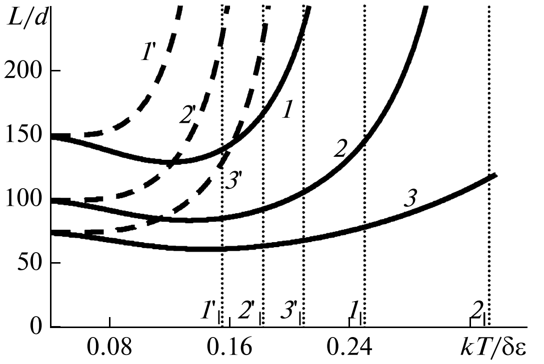

Fig. 8. Temperature dependences of the equilibrium L/d ratio at $\gamma = 0.2$ eV (*1*–*3*) and 0.1 eV (*1'*–*3'*) and different alloy compositions: $c_0 = 0.02$ (*1*, *1'*), 0.03 (*2*, *2'*), and 0.04 (*3*, *3'*). The dashed lines denote the temperatures at which the equilibrium L/d ratio disappears at the corresponding parameters.

the scenario of an interrupted decomposition [47]. As mentioned above, in small grains, the impurity in the bulk is exhausted. As a result, isolated segregations remain on the GB at equilibrium and the notion of GB concentration loses its sense. Thus the Fowler equation can be used to predict the possibility of a GB transition, but the solution is physically inadequate for small grains.

A more correct study of GB transition can be performed on the basis of the formulated approach by numerical simulation using the Cahn–Hilliard spinodal decomposition model, which takes into account the local change in the interatomic interaction energies (ε, ν) near the GB [11–13]. The result (the morphology of segregations on the GB) should evidently depend on the ratio of the energies $\delta\varepsilon$, $\delta\nu$, ε, and ν. This problem requires the use of diffusion kinetics equations and is beyond the scope of this study.

Equilibrium Boundary Width and Grain Size

The peculiarities of GBS considered in previous sections refer to systems with fixed grain size and grain boundary. As is well known, recrystallization occurs in pure metals and is described by the Hillert equation [53], which coincides in its structure with the Livshits–Slezov equation for seed growth [54]. The motive force of recrystallization is the decrease in the total energy of intergrain boundaries due to an increase in the average grain size. Therefore, recrystallization occurs irreversibly up to a transition to a single crystal, but the kinetics of this process, which depends on the number of atomic jumps across the boundary and the boundary curvature, slows down at lower temperatures and larger grain sizes. Hence it follows that the above results obtained for the fixed L/d ratio can be interpreted as quasistationary states achieved in the course of the permanent fragmentation of grains at a temperature T followed by fast quenching to the temperatures at which the diffusion (and hence recrystallization) is frozen.

It was noticed [55] that while decreasing the free energy of the system, GBSs can stabilize the grain structure in contrast to the expected Livshits–Slezov kinetics. This conclusion was confirmed by both experimental [9, 56–58] and numerical simulation [59] data. A molecular dynamics simulation showed that in a system with Lennard-Jones potentials, the energy of a GB can become zero if it accommodates a sufficient number of atoms; i.e., the presence of a GB in the system becomes thermodynamically favorable due to segregations. The equilibrium grain size L_{eq} was determined within the framework of a statistical approach using Fowler equation (2) [46, 60]. It was recently shown [8] that L_{eq} quickly increases as the mean composition of the alloy decreases; the theoretical predictions were in good agreement with the experimental data for Ni–P and Ni–W systems.

Researchers generally tend to consider the grain size L as the free parameter. The equation for the free energy minimum, however, contains the dimensionless d/L ratio. Consequently, the energy minimization can be provided not only by optimization of L at a fixed GB width, but also by optimization of d at fixed L, or by varying these quantities together. Indeed, let us imagine, for simplicity, that the volume of the sample V_0 is filled with equal grains, the volume of each grain being equivalent to the volume of a sphere with a radius L and a boundary layer with a width d. Then the number of grains in the volume V_0 is inversely proportional to the volume of the sphere and the equation for the free energy of the sample is recorded as

$$\begin{gathered} F(\tilde{d})/V_0 = (1-\tilde{d})^3 f(c_b(\tilde{d})) \\ + (1-(1-\tilde{d})^3)[f(c_{\text{GB}}(\tilde{d})) + \gamma], \qquad (15) \\ \tilde{d} = d/L, \end{gathered}$$

where γ is the energy density of the GB layer in the absence of an impurity; $f(c_b)$ and $f(c_{\text{GB}})$ are the free energy densities of the alloy calculated by (3) at concentrations in the bulk and on GB. According to (3) and (15), the free energy of the sample depends on the dimensionless ratio of parameters $\tilde{d} = d/L$. This allows us to suggest a mechanism of stabilization of the nonequilibrium grain boundaries due to the formation of a wide segregation layer.

The nonequilibrium GBs appear under the conditions of severe plastic deformation of a material at small grain sizes (10–100 nm) and are characterized by strong lattice distortions in a layer with a width of several nanometers [24]. The kinetic factors (dislocation or vacancy flows) may be the reason for segregations on such boundaries during SPD. The above considerations, however, suggest that the nonequilibrium segregations that appeared on the nonequilibrium grain boundaries lead to a decrease in the GB energy and are stabilized; i.e., the defective structure of the boundary and the segregation layer that appeared on it

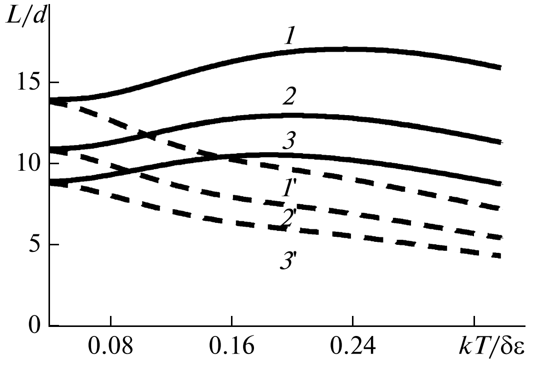

Fig. 9. Temperature dependences of the equilibrium L/d ratio at $\gamma = 0.2$ eV (*1–3*) and 0.1 eV (*1'–3'*) and different alloy compositions: $c_0 = 0.20$ (*1, 1'*), 0.25 (*2, 2'*), and 0.30 (*3, 3'*).

acquire equilibrium properties. In this case, further fragmentation of grains is disadvantageous because the minimum $F(d/L)$ was achieved due to an increase in the equilibrium d rather than a decrease in the equilibrium L. It is reasonably believed that suppression of wide segregations should promote further fragmentation of the grain structure.

Figures 8 and 9 present the plots of the temperature dependence of the equilibrium L/d ratio for the ideal solid solution at different alloy composition and intrinsic boundary energy. The plots were constructed using Eqs. (3) and (15). The curves are generally nonmonotonous; at moderate T, a minimum of L/d is reached for dilute solutions (Fig. 8) and a maximum for concentrated solutions (Fig. 9). In dilute solid solutions, the equilibrium L/d ratio exists only below the critical temperature and quickly decreases as the impurity concentration increases.

CONCLUSIONS

At moderate temperatures, a critical grain size exists in nanocrystalline alloys at which the integrated degree of decomposition reaches maximum. The indicated critical grain size increases as the average (over the sample) impurity concentration decreases. In multicomponent alloys, the GB impurity concentration with a lower segregation energy reaches maximum at a certain grain size. For the segregation kinetics in nanocrystalline alloys, an approximate analytical solution was suggested. The equilibrium grain size exists below a critical temperature and its temperature dependence is generally nonmonotonous. A hypothesis was put forward according to which the appearance of nonequilibrium grain boundaries hinders further fragmentation of alloy grains under the conditions of severe plastic deformation.

ACKNOWLEDGMENTS

The author is grateful to Profs. A.E. Ermakov and Yu.N. Gornostyrev for useful discussions that stimulated the writing of this paper.

REFERENCES

1. K. Wang, T. Xu, C. Shao, and C. Yang, J. Iron Steel Res. **18** (6), 61 (2011).
2. X. F. Zhang, T. Fujita, D. Pan, et al., Mater. Sci. Eng. A **527**, 2297 (2010).
3. C. Y. Wong, C. R. M. Grovenor, P. E. Batson, and D. A. Smith, J. Appl. Phys. **57**, 438 (1985).
4. Y. Fujita, K. Kitakizaki, and K. Masuda-Jindo, Solid State Phenom. **51–52**, 21 (1996).
5. V. I. Arkharov, in *The Physics of Brittle Fracture* (Naukova Dumka, Kiev, 1976) [in Russian].
6. A. V. Vasil'ev, S. B. Ermakov, and V. V. Karginova, Kholodil. Tekh. Konditsion., No. 1, 16 (2009).
7. D. L. Beke, C. Cserháti, and I. A. Szabó, J. Appl. Phys. **95**, 4996 (2004).
8. J. R. Trelewicz and C. A. Schuh, Phys. Rev. B **79**, 094112 (2009).
9. X. Sauvage, A. Ganeev, Yu. Ivanisenko, et al., Adv. Eng. Mater. **14**, 968 (2012).
10. B. S. Bokshtein, Ch. V. Kopetskii, L. S. Shvindlerman, et al., in *Structure and Properties of Inner Surfaces of Division in Metals* (Nauka, Moscow, 1988) [in Russian].
11. Yu. N. Gornostyrev, I. K. Razumov, and A. Ye. Yermakov, J. Mater. Sci. **39**, 5003 (2004).
12. I. K. Razumov, Yu. N. Gornostyrev, and A. Ye. Yermakov, J. Alloys Compd. **434–435**, 535 (2007).
13. I. K. Razumov, Yu. N. Gornostyrev, and A. Ye. Yermakov, Rev. Adv. Mater. Sci. **18**, 767 (2008).
14. P. Lejcek, *Grain Boundary Segregation in Metals*, Springer Series in Materials Science, Vol. 136 (Springer, 2010).
15. G. P. Vyatkin and T. P. Privalova, *Surface Segregation and Desorption under Phase Transitions in Metals* (Chelyab. Gos. Tekh. Univ., Chelyabinsk, 1996) [in Russian].
16. B. S. Bokshtein, Ch. V. Kopetskii, and L. S. Shvindlerman, *Thermodynamics and Kinetics of Grain Boundaries in Metals* (Metallurgiya, Moscow, 1986) [in Russian].
17. D. McLean, *Grain Boundaries in Metals* (Clarendon, Oxford, 1957; Metallurgizdat, Moscow, 1960).
18. R. H. Fowler and E. A. Guggenheim, *Statistical Thermodynamics* (Cambridge Univ. Press, 1939).
19. V. V. Slezov, L. N. Davydov, and V. V. Rogozhkin, Phys. Solid State **37**, 1964 (1995).
20. *Phase Transformations during Irradiation*, Ed. by F. V. Nolfi (Applied Science Publisher, London, 1983; Metallurgiya, Chelyabinsk, 1989).
21. I. K. Razumov, V. L. Gapontsev, Yu. N. Gornostyrev, et al., Phys. Met. Metallogr. **96**, 351 (2003).
22. X. Sauvage, G. Wilde, S. V. Divinski, et al., Mater. Sci. Eng. A **540**, 1 (2012).
23. I. K. Razumov, Kondens. Sredy Mezhfaz. Granitsy **12**, 394 (2010).

24. R. Z. Valiev and I. V. Aleksandrov, *Nanostructured Materials Produced by Severe Plastic Deformation* (Logos, Moscow, 2000) [in Russian].
25. R. Z. Valiev, R. K. Islamgaliev, and I. V. Alexandrov, Prog. Mat. Sci. **45**, 103 (2000).
26. A. E. Ermakov, Fiz. Met. Metalloved., No. 11, 4 (1991).
27. H. Bakker, P. I. Loeff, and A. W. Weeber, Def. Diff. Forum **66**, 1169 (1989).
28. H. Bakker, G. F. Zhou, and H. Yang, Progress Mater. Sci. **39**, 159 (1995).
29. U. Czubayko, N. Wanderka, V. Naundorf, et al., Mater. Sci. Eng. A **327**, 54 (2002).
30. C. Bansal, Z. Q. Gao, L. B. Hong, and B. Fultz, J. Appl. Phys. **76**, 5961 (1994).
31. A. I. Deryagin, V. A. Zavalishin, V. V. Sagaradze, and A. R. Kuznetsov, Phys. Met. Metallogr. **89**, 610 (2000).
32. A. V. Korolev, E. G. Gerasimov, V. A. Kazantsev, and A. I. Deryagin, Fiz. Met. Metalloved. **79**, 136 (1995).
33. T. C. E. Rodriquez, F. N. Sanches, and Z. L. A. Mendoza, Phys. Rev. B **51**, 12142 (1995).
34. V. S. Gaviko, A. G. Popov, A. S. Ermolenko, et al., Phys. Met. Metallogr. **92**, 158 (2001).
35. V. L. Gapontsev, A. I. Deryagin, and T. M. Gapontseva, Fiz. Mezomekh. **12** (6), 53 (2009).
36. V. A. Shabashov, S. V. Borisov, A. E. Zamatovskii, et al., Phys. Met. Metallogr. **102**, 545 (2006).
37. I. K. Razumov, Russ. J. Phys. Chem. A **84**, 1485 (2010).
38. R. W. Siegel, in *Materials Interfaces: Atomic-Level Structure and Properties*, Ed. by D. Wolf and S. Yip (Chapman Hall, London, 1992).
39. K. Ishida, J. Alloys Compd. **235**, 244 (1996).
40. C. Lea and M. P. Seah, Scr. Metall. **9**, 573 (1975).
41. M. T. Thomas, D. R. Baer, R. H. Jones, and S. M. Bruemmer, J. Vac. Sci. Technol. **17**, 22 (1980).
42. H. J. Grabke, Steel Res. **57**, 178 (1986).
43. M. P. Seah and E. D. Hondros, Proc. R. Soc. London, Ser. A **335**, 191 (1973).
44. E. D. Hondros and M. P. Seah, Int. Met. Rev. **22**, 267 (1977).
45. V. V. Slezov, L. N. Davydov, and V. V. Rogozhkin, Phys. Solid State **40**, 226 (1998).
46. Cs. Cserhati, I. A. Szabo, and D. L. Beke, J. Appl. Phys. **83**, 3021 (1998).
47. J. Christian, *The Theory of Transformations in Metals and Alloys. Equilibrium and General Kinetic Theory* (Pergamon, Oxford, 1975).
48. J. Weissmuller, Nanostruct. Mater. **3**, 261 (1993).
49. P. Gruffel and C. Carry, J. Eur. Ceram. Soc. **11**, 189 (1993).
50. S. V. Divinski, F. Hisker, Y.-S. Kang, et al., Acta Mater. **52**, 631 (2004).
51. A. D. Polyanin, *Handbook on Linear Equations of Mathematical Physics* (Fizmatlit, Moscow, 2001) [in Russian].
52. Ya. E. Geguzin, *Diffusion Zone* (Nauka, Moscow, 1979) [in Russian].
53. M. Hillert, Acta Metall. **13**, 227 (1965).
54. E. M. Lifshits and L. P. Pitaevskii, *Physical Kinetics* (Nauka, Moscow, 1979; Pergamon, Oxford, 1981).
55. J. Weissmuller, Nanostruct. Mater., No. 3, 261 (1993).
56. R. Kirchheim, Acta Mater. **50**, 413 (2002).
57. K. A. Darling, R. N. Chan, P. Z. Wong, et al., Scr. Mater. **59**, 530 (2008).
58. E. Botcharova, J. Freudenberg, and L. Schulz, Acta Mater. **54**, 3333 (2006).
59. P. C. Millett, R. P. Selvam, and A. Saxena, Acta Mater. **55**, 2329 (2007).
60. D. L. Beke, C. Cserhati, and I. A. Szabo, J. Appl. Phys. **95**, 4996 (2004).

Translated by L. Smolina